

Synthesis and Conformational Analysis of Locked Carbocyclic Analogues of 1,3-Diazepinone Riboside, a High-Affinity Cytidine Deaminase Inhibitor

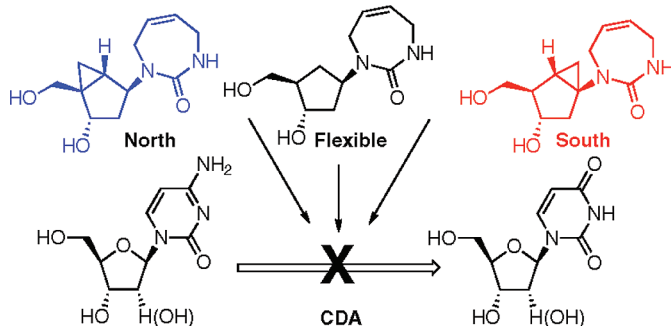
Olaf R. Ludek,[†] Gottfried K. Schroeder,^{‡,§} Chenzhong Liao,[†] Pamela L. Russ,[†]
Richard Wolfenden,[‡] and Victor E. Marquez*,[†]

[†]Laboratory of Medicinal Chemistry, Center for Cancer Research, National Cancer Institute at Frederick, National Institutes of Health, Frederick, Maryland 21702, and [‡]Department of Biochemistry and Biophysics, University of North Carolina, Chapel Hill, North Carolina 27599.

[§]Current address: University of Texas at Austin, Division of Medicinal Chemistry, College of Pharmacy, 1 University Station C0850, Austin, TX 78712.

marquezv@mail.nih.gov

Received June 2, 2009



Cytidine deaminase (CDA) catalyzes the deamination of cytidine via a hydrated transition-state intermediate that results from the nucleophilic attack of zinc-bound water at the active site. Nucleoside analogues where the leaving NH_3^+ group is replaced by a proton and prevent conversion of the transition state to product are very potent inhibitors of the enzyme. However, stable carbocyclic versions of these analogues are less effective as the role of the ribose in facilitating formation of hydrated species is abolished. The discovery that a 1,3-diazepinone riboside (**4**) operated as a tight-binding inhibitor of CDA independent of hydration provided the opportunity to study novel inhibitors built as conformationally locked, carbocyclic 1,3-diazepinone nucleosides to determine the enzyme's conformational preference for a specific form of sugar pucker. This work describes the synthesis of two target bicyclo[3.1.0]hexane nucleosides, locked as north (**5**) and south (**6**) conformers, as well as a flexible analogue (**7**) built with a cyclopentane ring. The seven-membered 1,3-diazepinone ring in all the three targets was built from the corresponding benzoyl-protected carbocyclic bis-allyl ureas by ring-closing metathesis. The results demonstrate CDA's binding preference for a south sugar pucker in agreement with the high-resolution crystal structures of other CDA inhibitors bound at the active site.

Introduction

Cytidine deaminase (CDA; EC 3.5.4.5) is a zinc-dependent enzyme that catalyzes the deamination of cytidine to uridine via the formation of an unstable, hydrated transition-state

(ts) intermediate (Figure 1).¹ The spontaneous deamination of cytidine is very slow and proceeds with a rate constant around 10^{-10} s^{-1} , however, the enzyme is able to accelerate the rate of deamination by an impressive 12–14 orders of magnitude.² This tremendous enhancement reflects an extraordinary affinity for the hydrated intermediate

(1) Cacciamani, T.; Vita, A.; Cristalli, G.; Vincenzetti, S.; Natalini, P.; Ruggieri, S.; Amici, A.; Magni, G. *Arch. Biochem. Biophys.* **1991**, 290, 285–292.

(2) Schroeder, G. K.; Wolfenden, R. *Biochemistry* **2007**, 46, 13638–13647.

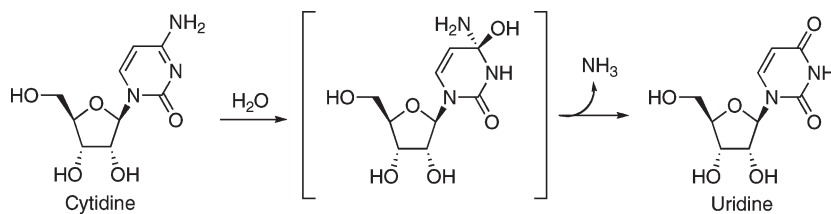
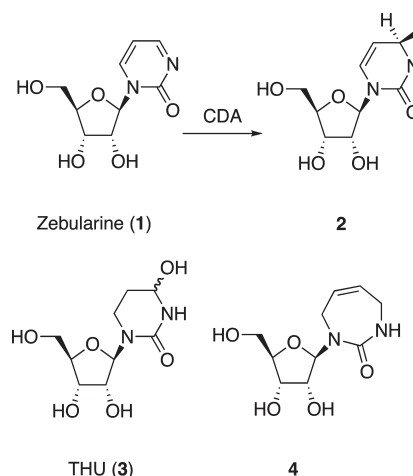


FIGURE 1. Transition state for the hydrolytic deamination of cytidine.

($K_{ts} \sim 10^{-16}$ M).^{3a} Formation of such a hydrated intermediate has been confirmed biochemically^{3b, 3c} and by the crystal structure of the inhibitor zebularine (**1**) bound to CDA, which revealed the formation of the 3,4-double-bond hydrate (**2**) at the active site.^{3d} Inhibition of CDA is of particular interest therapeutically to enhance the activity of readily deaminated antitumor nucleosides such as cytosine arabinoside and 5-aza-2'-deoxycytidine.⁴



Another well-known inhibitor of CDA is tetrahydrouridine (**3**, THU), which despite lacking the 5,6-double bond of the hydrated zebularine ring possesses a hemiaminal structure that embodies the properties of a powerful transition-state mimic. Indeed, a recent, high-resolution crystal structure of mouse CDA complexed with THU shows the active diastereoisomer with the 4-OH group spatially oriented toward the zinc ion.⁵

An intriguing molecule, also displaying a strong inhibition of CDA ($K_i = 25$ nM), but for which the mechanism of action remained unexplained for many years, is the diazepinone ribose **4**.⁶ This compound possesses a critical double bond, but as opposed to the hydrated 3,4-double of zebularine and the hemiaminal functionality of THU, it lacks any possibility of interacting with CDA via zinc coordination. Fourteen years later, after solving the crystal structure of human CDA bound to the diazepinone ribose **4**, Verdine et al. demonstrated that the mode of action of this tight-binding inhibitor

was indeed wholly independent from a hydration mechanism and showed instead that the strong binding at the active site resulted from the edge-on $\pi-\pi$ interaction between the diazepinone ring's double bond and Phe137.⁷

For these three molecules, zebularine (**1**), THU (**3**), and diazepinone riboside (**4**), it is clear that the interactions of the nucleobase with the active site are critical for strong binding, and not surprisingly, the majority of the structure–activity-relationship (SAR) studies reported to date for CDA deal almost exclusively with changes in the heterocyclic base. In terms of the role of the sugar moiety, however, fewer studies have been conducted. Even though the sugar ring has a small effect on the rate of the spontaneous deamination reaction of cytidine, it greatly enhances the reactivity of the enzymatic reaction by increasing the effective concentration of the altered substrate at the active site.⁸ Such an entropic advantage is the direct result of the parts (base and ribose) being properly connected to fit the active site.

The critical parameter of the ribose (or 2'-deoxyribose) that ensures that the interactions between the parts are optimal is the sugar pucker, which is defined by the pseudorotational phase angle P .⁹ Normally, conventional nucleosides in solution undergo rapid equilibration between ranges of P defined by two main twist furanose puckering domains centered around a ³T₂ (north-type) and a ²T₃ (south-type) conformation. Despite the small difference in energy between these two conformations, an emerging picture from recent observations is that the majority of nucleoside(tide) target enzymes, whether anabolic or catabolic, appear to have strict conformational requirements for substrate binding, accepting the furanose ring only in a particular, well-defined shape.¹⁰ Because the value of P and the corresponding glycosyl torsion angle χ are interdependent, with the latter responding in a concerted manner to minimize steric clashes, the value of χ is also of critical importance for the two connecting pieces to provide optimal recognition.

In the specific case of CDA, the crystal structures of the enzyme bound to zebularine hydrate (**2**), THU (**3**), and diazepinone riboside (**4**) show the conformation of the sugar ring in the south hemisphere, close to a 2'-endo conformation. In particular, the 1.48 Å resolution structure by Kumakasa et al.⁵ shows the ribose ring of THU clearly in a south conformation with the 3'-OH hydrogen bonded to the side

(3) (a) Snider, M. J.; Wolfenden, R. *Biochemistry* **2001**, *40*, 11364–11371. (b) Frick, L.; Yang, C.; Marquez, V. E.; Wolfenden, R. *Biochemistry* **1989**, *28*, 9423–9430. (c) Xiang, S.; Short, S. A.; Wolfenden, R.; Carter, C. W., Jr. *Biochemistry* **1995**, *34*, 4516–4523. (d) Betts, L.; Xiang, S.; Short, S. A.; Wolfenden, R.; Carter, C. W., Jr. *J. Mol. Biol.* **1994**, *235*, 635–656.

(4) (a) Laliberte, J.; Marquez, V. E.; Momparler, R. L. *Cancer Chemother. Pharmacol.* **1992**, *30*, 7–11. (b) Lemaire, M.; Momparler, R. L. F.; Bernstein, M.; Marquez, V. E.; Momparler, R. L. *Anti-Cancer Drugs* **2005**, *16*, 301–308.

(5) Teh, A.-H.; Kimura, M.; Yamamoto, M.; Tanaka, N.; Yamaguchi, I.; Kumasaka, T. *Biochemistry* **2006**, *45*, 7825–7833.

(6) Liu, P. S.; Marquez, V. E.; Driscoll, J. S.; Fuller, R. W. *J. Med. Chem.* **1981**, *24*, 662–666.

(7) Chung, S. J.; Fromme, C.; Verdine, G. L. *J. Med. Chem.* **2005**, *48*, 658–660.

(8) Carlow, D. C.; Short, S. A.; Wolfenden, R. *Biochemistry* **1998**, *37*, 1199–2103.

(9) Saenger, W. *Principles in Nucleic Acid Structure*; Springer-Verlag: New York, 1984.

(10) Marquez, V. E. The Properties of Locked Methanocarba Nucleosides in Biochemistry, Biotechnology, and Medicinal Chemistry. In *Modified Nucleosides in Biochemistry, Biotechnology and Medicine*; Herdewijn, Ed.; Wiley-VCH Verlag GmbH & Co. KGaA: Weinheim, 2008; Chapter 12, pp 307–341 (ISBN 978-3-527-31820-9).

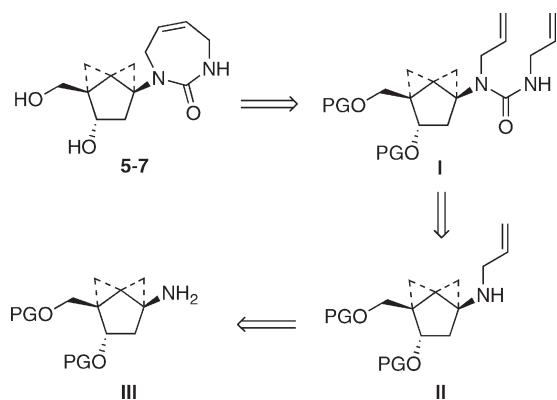


FIGURE 2. Retrosynthetic analysis of the target compounds **5–7** (PG = protecting group).

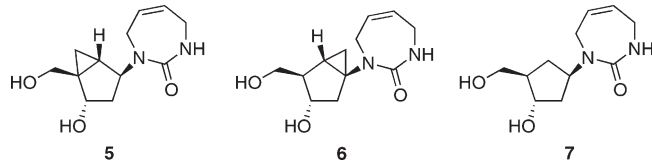
chains of highly conserved Asn54 and Glu56. Using our interactive tool, PROSIT,¹¹ which calculates the pseudorotational parameters of nucleosides and nucleotides bound to proteins, we calculated a value of $P = 158.55^\circ$ (2'-endo) for THU which is clearly in the south hemisphere. Other parameters calculated included the maximum puckering amplitude ($\nu_{\max} = 36.68^\circ$) and the glycosyl torsion angle of the tetrahydrouracil ring, which is in the anti range ($\chi = -136.51^\circ$). Similarly, the conformational parameters for the bound diazepinone riboside (**4**)⁷ calculated by PROSIT matched very closely those of THU ($P = 158.18^\circ$, $\nu_{\max} = 32.10^\circ$, and $\chi = -149.66^\circ$).

The unique preference of CDA for the south (2'-endo) conformation stands in sharp contrast with the related purine deaminase, adenosine deaminase (ADA), which prefers to bind both substrate and inhibitors in the antipodal north (3'-endo) conformation.¹² Despite the similarity of the mechanisms of deamination, which in both enzymes proceed via analogous tetrahedral intermediates, the secondary and tertiary structural motifs of the two enzymes are completely unrelated and lack any evolutionary homology.¹³

With the aim of studying the impact that the sugar conformation has on CDA, and how it might impinge on the other critical interactions with important residues at the active site that are *independent of zinc binding, and thus not controlled by the chemical generation of an unstable, chiral hydrated intermediate*, we chose the diazepinone riboside **4** as a prototype. This diazepinone riboside preserves all the other critical interactions with conserved amino acids, such as Glu56 and Asn64, plus the CONH portion of the diazepinone ring forms a similar set of hydrogen bonds with Ala66 and Glu67 at the active site that are seen with the nucleobases of the hydrate of zebularine and with THU. The only difference is the pronounced wrinkle of the seven-membered ring in **4**, which juts the double bond out of plane and allows it to interact with the π -face of Phe137 via a canonical π/π -interaction.⁷

In the present work, we report on the construction of conformationally locked north- (**5**) and south-diazepinone (**6**) riboside analogues of **4** built on a stable carbocyclic scaffold: the bicyclo[3.1.0]hexane template.¹⁴ Because

CDA accepts and deaminates efficiently both ribo and 2'-deoxyribonucleosides, we chose for simplicity to prepare 2'-deoxy versions of these carbocyclic nucleosides. For comparison, the plain and flexible cyclopentane analogue (**7**) was also synthesized; all of the compounds were evaluated as CDA inhibitors and compared with the parent riboside (**4**).



Results

Synthesis. To accomplish the syntheses of these compounds, we sought a linear strategy that could be adapted to all three targets. This approach differs from the convergent approach used for the synthesis of **4** in order to avoid problems with the likely formation N- and O-alkylated products.⁶ The retrosynthetic analysis used in the current approach shows how the 1,3-diazepin-2-one moiety is to be engendered by a ring-closing metathesis (RCM) reaction on the bis-allyl ureas (**I**) (Figure 2). These in turn could be accessed by the reaction of allyl isocyanate with the monoalkylated amines (**II**) derived from the appropriate carbocyclic primary amines (**III**).

The synthesis of the locked north-diazepinone nucleoside started with the known bicyclo[3.1.0]hexanol **8**.¹⁵ As shown in Scheme 1, conversion of **8** to its methanosulfonyl ester **9** was followed by nucleophilic attack with sodium azide to give **10** with inversion of stereochemistry. Alternatively, alcohol **8** was reacted with diphenylphosphoryl azide (DPPA) in DMF to give directly the desired azide **10**.¹⁶ After hydrogenolysis over Lindlar's catalyst, the azide was quantitatively reduced to the key intermediate amine **11**, and alkylation of the primary amine with allyl bromide in DMF, with either K_2CO_3 or Cs_2CO_3 as catalysts, gave the monoalkylated amine **12** in 35 and 33% yield, respectively, showing no clear advantage with the use of Cs_2CO_3 .¹⁷

A change in strategy involving the reduction of the azide **11** in the presence of di-*tert*-butyl dicarbonate (Scheme 2) led to the Boc-protected amine **14**,¹⁸ which was selectively alkylated with allyl bromide and potassium hexamethyldisilazide in DMF to give **15**. Removal of the Boc group with TFA led to the monoallylated amine **12**, which reacted with allylisocyanate to form the desired diallylurea **16**. Unfortunately, all attempts to form the seven-membered cyclic urea **17** via RCM¹⁹ with

(15) Yoshimura, Y.; Moon, H. R.; Choi, Y. S.; Marquez, V. E. *J. Org. Chem.* **2002**, *67*, 5938–5945.

(16) (a) Hernandez, S.; Ford, H. Jr; Marquez, V. E. *Bioorg. Med. Chem.* **2002**, *10*, 2723–2730. (b) Wolff, O.; Waldvogel, S. R. *Synthesis* **2004**, *8*, 1303–1305.

(17) (a) Salvatore, R. N.; Nagle, A. S.; Schmidt, S. E.; Jung, K. W. *Org. Lett.* **1999**, *1*, 1893–1896. (b) Salvatore, R. N.; Nagle, A. S.; Jung, K. W. *J. Org. Chem.* **2002**, *67*, 674–683.

(18) (a) Saito, S.; Nakajima, H.; Inaba, M.; Moriwake, T. *Tetrahedron Lett.* **1989**, *30*, 837–838. (b) Evans, D. A.; Evrard, D. A.; Rychnevsky, S. D.; Früh, T.; Whittingham, W. G.; DeVries, K. M. *Tetrahedron Lett.* **1992**, *33*, 1189–1192.

(19) (a) Miller, S. J.; Kim, S.-H.; Chen, Z.-R.; Grubbs, R. H. *J. Am. Chem. Soc.* **1995**, *117*, 2108–2109. (b) Martin, S. F.; Follows, B. C.; Hergenrother, P. J.; Franklin, C. L. *J. Org. Chem.* **2000**, *65*, 4509–4514. (c) Hoffmann, R. V.; Madan, S. *J. Org. Chem.* **2003**, *68*, 4876–4885. (d) Winkler, J. D.; Asselin, S. M.; Shepard, S.; Yuang, J. *Org. Lett.* **2004**, *6*, 3821–3824. (e) Gracias, V.; Gasiecki, A. F.; Djuric, S. W. *Org. Lett.* **2005**, *7*, 3183–3186. (f) Dougherty, J. M.; Jimenez, M.; Hanson, P. R. *Tetrahedron* **2005**, *61*, 6218–6230. (g) Tao, Z.-F.; Chen, Z.; Bui, M.-H.; Kovar, P.; Johnson, E.; Bouska, J.; Zhang, H.; Rosenberg, S.; Sowin, T.; Lin, N.-H. *Bioorg. Med. Chem. Lett.* **2007**, *17*, 6593–6601.

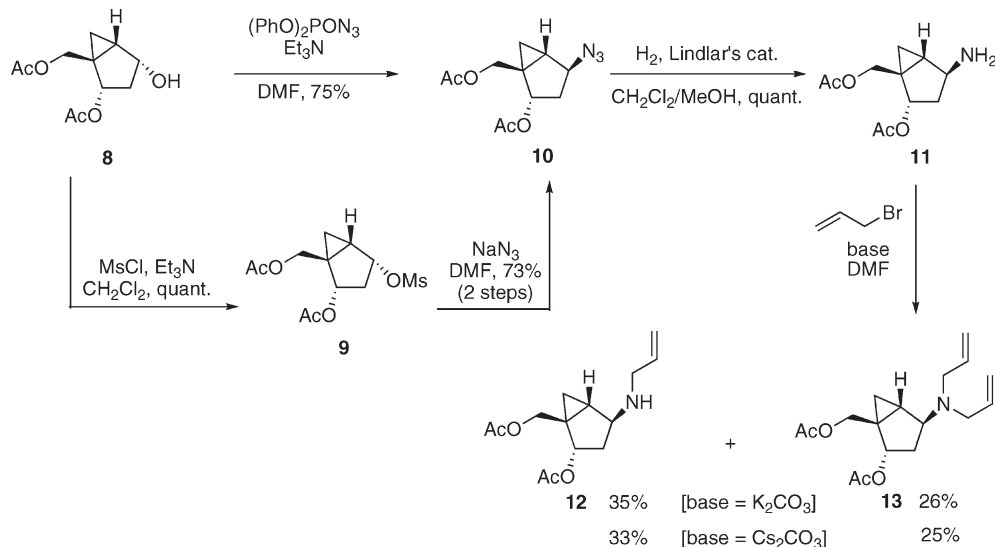
(11) Sun, G.; Voigt, J. H.; Filippov, I. G.; Marquez, V. E.; Nicklaus, M. C. *J. Chem. Inf. Comput. Sci.* **2004**, *44*, 1752–1762.

(12) Wang, Z.; Quirocho, F. A. *Biochemistry* **1998**, *37*, 8314–8324.

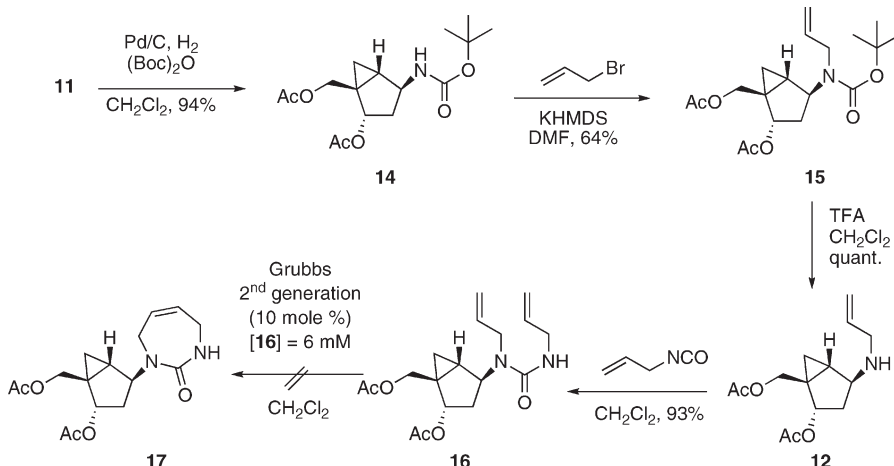
(13) Carter, C. W., Jr. *Biochimie* **1995**, *77*, 92–98.

(14) Part of this work was presented as a poster at the XVIII International Round Table for Nucleosides, Nucleotides and Nucleic Acids, Kyoto, Japan, Sep 8–11, 2008: Ludek, O. R.; Schroeder, G. K.; Wolfenden, R.; Marquez, V. E. *Nucleic Acids Symp. Series No. 52*, **2008**, 659–660.

SCHEME 1



SCHEME 2



Grubbs's second-generation catalysts at room temperature or reflux in either CH_2Cl_2 or toluene failed and only starting material was recovered.

We surmised that the failure of the metathesis reaction was due to the unfavorable orientation of the allyl groups in **16**, which prevented the intramolecular condensation.^{19c} At 6 mM substrate concentration no cross-metathesis products were observed either. After considering the equilibrium between the *cis*- and *trans*-configurations of the amide, we realized that the expected, more stable *trans*-configuration would indeed place the allyl groups away from each other making ring closure impossible (Figure 3).

Since Kaválek et al. have demonstrated that the *cis/trans*-isomerization barrier can be significantly lowered by alkylation of the amide,²⁰ we considered that such equilibrium could be tunable by using a suitably protected amide group. As a first attempt, the amide moiety was silylated with hexamethyldisilazane and ammonium sulfate as catalyst to give the aza-enol ether **18** in quantitative yield, where the

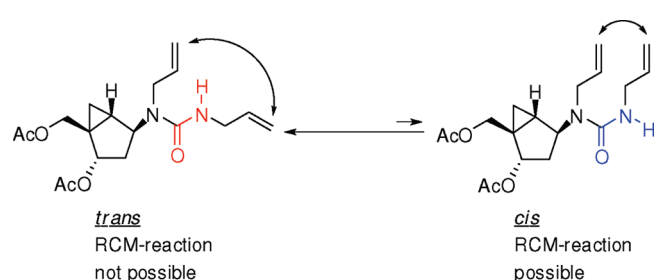
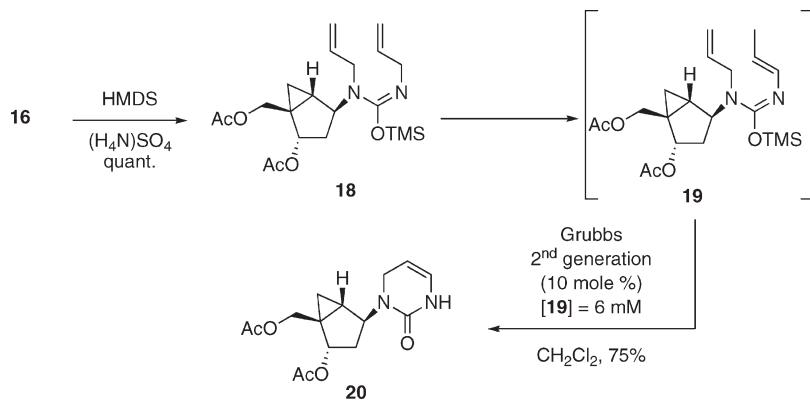


FIGURE 3. Equilibrium between the *cis*- and *trans*-conformations of the amide bond in **16**.

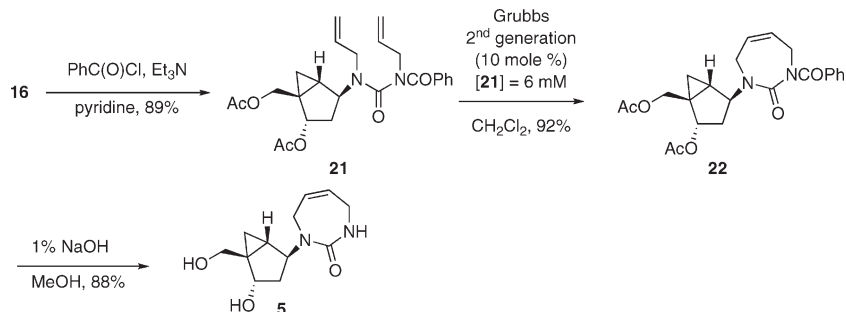
bulky trimethylsilyl group was expected to favor a desirable conformational change (Scheme 3). Because of the moisture sensitivity expected for this class of silylated compounds, the RCM reaction was performed immediately with Grubbs second-generation catalyst under reflux in methylene chloride to give, according to TLC analysis, a single product after 30 min. Unfortunately, the expected seven-membered ring was not formed and instead the six-membered urea **20** was obtained in 75% yield. Although the formation of **20** was

(20) Kaválek, J.; Macháček, V.; Svobodá, G.; Štěrba, V. *Collect. Czech. Chem. Commun.* **1987**, 52, 1999–2004.

SCHEME 3



SCHEME 4



disappointing, a result that most likely happened due to the isomerization of the double bond to form the *s-cis* conjugated π -system,²¹ the isolation of a cyclic product proved that a *cis*-geometry was essential for the success of the RCM reaction.

Encouraged by these results, we then investigated the effect of a simple acyl group for the RCM reaction, which would allow for the easy removal of all protecting groups in one step. Therefore, urea **16** was acylated with benzoyl chloride in pyridine to form the UV-active urea **21** in 89% yield. Interestingly, the introduction of the benzoyl group led to significant broadening of some signals in the proton and carbon NMR spectra. The RCM reaction, performed under the same conditions as with **18**, smoothly afforded the desired seven-membered ring in 92%, thus confirming the role of the stereochemistry of the urea in the intramolecular cyclization. Finally, after global deprotection of the acyl groups, achieved with 1% NaOH solution in MeOH , the target structure **5** was obtained in excellent yield (Scheme 4).

The optimized reaction conditions for the synthesis of the conformationally locked north-diazepinone **5** were applied to the syntheses of both south and flexible targets (**6** and **7**), respectively (Scheme 5). Starting from enantiomerically pure **23**²² for the flexible analogue, mesylation and subsequent nucleophilic substitution with azide afforded compound **24** in 78% yield (two steps). Reduction of the azido group with

Lindlar's catalyst²³ in the presence of Boc-anhydride gave the Boc-protected amine **26b**. Similarly, reaction of the enantiomerically pure amine **25**²⁴ with Boc-anhydride gave the protected amine **26a**. From this point onward, the two approaches converge and the reactions and yields obtained for the penultimate intermediates **32a** and **32b** were essentially identical to those obtained before. The final removal of the benzyl protecting groups proceeded uneventfully in the presence of BCl_3 to give the target compounds **6** and **7**.

Kinetic Analysis of Carbocyclic Diazepinones as Inhibitors of Cytidine Deaminase. Cytidine deaminase activity was measured spectrophotometrically by following the loss of absorbance of cytidine at 282 nm ($\Delta\varepsilon = -3600$) in 0.1 M phosphate buffer (pH 6.8) at 25 °C. Concentrations of stock solutions of the three carbocyclic diazepinones were determined by proton NMR (see the Supporting Information Figures 1–3) in reference to a known concentration of pyrazine (10^{-3} M) added as an integration standard. Initial rates for the deamination of cytidine in the presence of all three inhibitors were determined and plotted as a function of $[\text{S}]$ vs $[\text{S}]/v_i$ (Hanes plot, Figures 4 and 5). Inhibition constants (K_i) for the three inhibitors (Table 1) were calculated using the following equation

$$K_i = \frac{[i]}{(K_M^{\text{app}}/K_M) - 1}$$

where K_M^{app} is the apparent value of the Michaelis constant (K_M) when measured in the presence of an inhibitor. Values

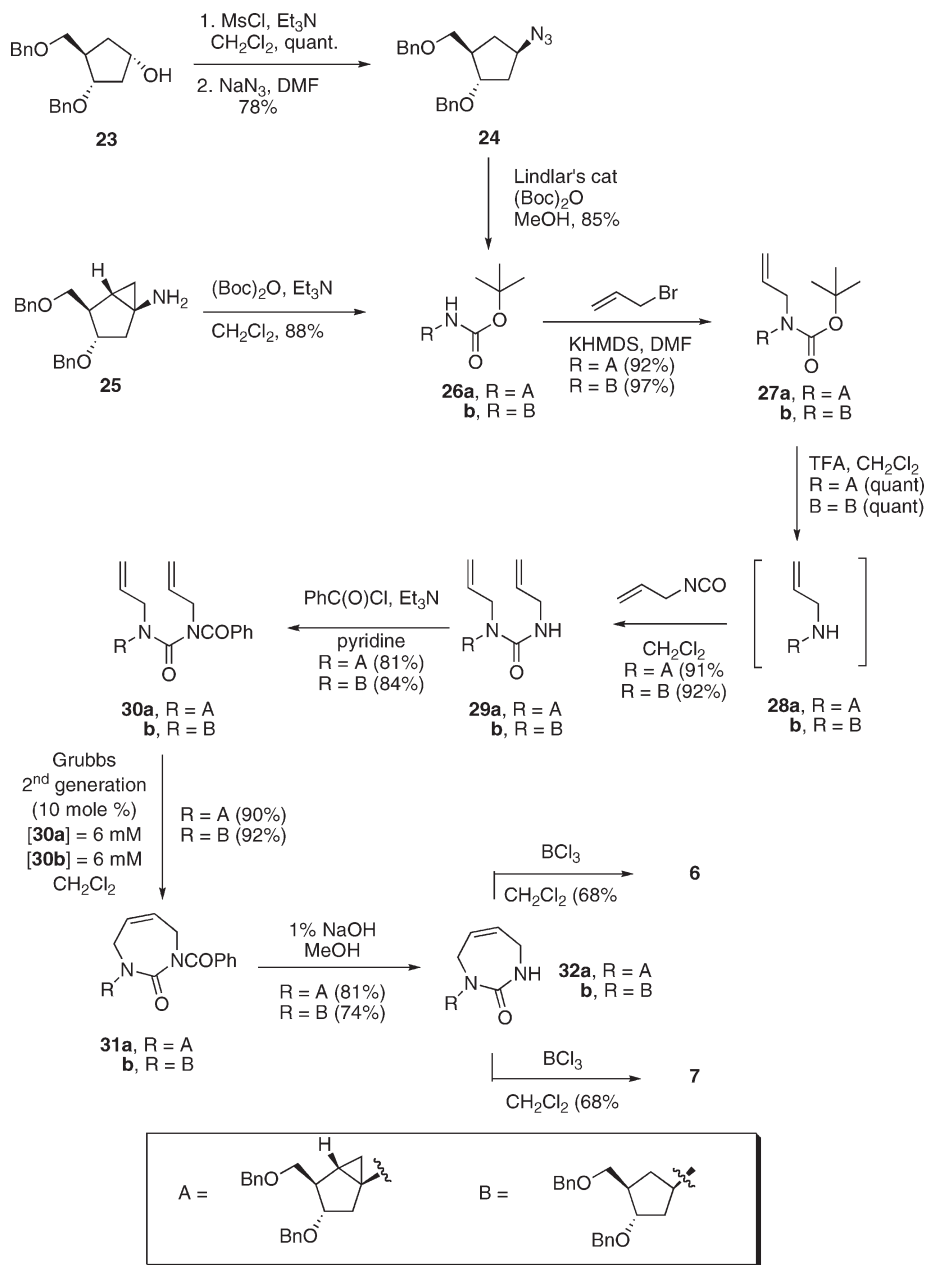
(21) (a) Hong, S. H.; Sanders, D. P.; Lee, C. W.; Grubbs, R. H. *J. Am. Chem. Soc.* **2005**, *127*, 17160–17161. (b) Schmidt, B. *J. Mol. Catal. A: Chem.* **2006**, *254*, 53–57. (c) Gimeno, N.; Formentín, P.; Steinke, J. H. G.; Vilar, R. *Eur. J. Org. Chem.* **2007**, 918–924. (d) Schmidt, B.; Biernat, A. *Org. Lett.* **2008**, *10*, 105–108. (e) Krompiec, S.; Krompiec, M.; Penczek, R.; Ignasiak, H. *Coord. Chem. Rev.* **2008**, *252*, 1819–1841.

(22) (a) Ludek, O. R.; Meier, C. *Synthesis* **2003**, *13*, 2101–2109. (b) Ludek, O. R.; Balzarini, J.; Krämer, T.; Meier, C. *Synthesis* **2006**, *8*, 1313–1324.

(23) Reddy, P. G.; Pratap, T. V.; Kumar, G. D. K.; Mohanty, S. K.; Baskaran, S. *Eur. J. Org. Chem.* **2002**, 3740–3743.

(24) Ezzitouni, A.; Barchi, J. J., Jr.; Marquez, V. E. *J. Chem. Soc., Perkin Trans. 1* **1997**, 1073–1078.

SCHEME 5



for K_M^{app} at various concentrations of inhibitor were estimated from the Hanes plots (Figures 4 and 5), which have $-K_M$ as the intercept on the [S] axis.

Figure 4 shows that both south (**6**) and north (**5**) carbocyclic diazepinones are competitive inhibitors of cytidine deaminase (parallel lines) and that the south derivative **6** is more potent than its north counterpart **5** (by a factor of ~ 2). Figure 5 shows that the flexible, carbocyclic diazepinone is also a competitive inhibitor, which surprisingly, as indicated in Table 1, is significantly more potent than either one of the locked derivatives. This compound, however, is still 16-fold less potent than the corresponding riboside **4**.⁶

Molecular Modeling. Molecular dynamics calculations and docking of the new carbocyclic diazepinone nucleosides (**5–7**) at the active site of CDA were based on the available crystal structure of human CDA bound to the diazepinone

riboside **4** (PDB ID: 1MQ0).⁷ The structures of the locked north- and south-diazepinone nucleosides (**5** and **6**) were constructed by importing the bicyclo[3.1.0]hexane templates from the crystal structures of north- (LETJEZ) and south- (YESMIS) bicyclo[3.1.0]hexane thymidine nucleosides which were downloaded from the Cambridge structural database (CCDC ConQuest version 1.5). The diazepinone ring as it appeared in the crystal structure of the CDA complexed with the diazepinone riboside **4** was mounted on the two bicyclo[3.1.0]hexane templates (see Figure 1 of the Supporting Information).

The diazepinone riboside **4** (Figure 6A) forms six hydrogen bonds (yellow dashed lines). Two hydrogen-bonding interactions are between the diazepinone ring and Glu67 (subunit C) and Ala66 (subunit C). The ribose ring forms the rest of the hydrogen bonds with Glu56 (subunit C), Asn54

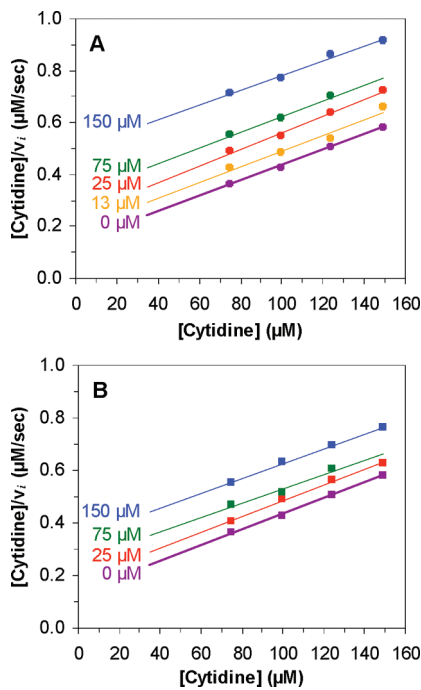


FIGURE 4. Hanes plot for cytidine deaminase activity at various concentrations (defined in the figure) of south/north carbocyclic diazepinone inhibitors. The parallel lines represent linear fits to the data and are indicative of competitive inhibition: (A) south-diazepinone **6** (●); (B) north-diazepinone **5** (■).

(subunit C), Ala58 (subunit D), and Tyr60 (subunit D). In addition, there is the important canonical π/π interaction with the π face of Phe137 (subunit A). The worst ligand, the north-diazepinone **5** (Figure 6B), maintains the hydrogen-bonding interactions of the diazepinone ring to Glu67 and Ala66, but the north-pseudosugar moiety forces the equatorially disposed 3'-OH to form a weaker hydrogen bond to Glu56. The 5'-OH cannot bind to Ala 58 or Tyr60 and reaches to Leu142 to form a new weak hydrogen bond. In addition, the interaction with Asn 54 is missing. The flexible diazepinone **7** (Figure 6C) and the south-diazepinone **6** (Figure 6D) form almost identical interactions. However, the hydrogen-bonding interactions of the 3'-OH in the flexible compound **7** (1.682 and 1.795 Å) appear to be stronger than those in the locked south-diazepinone **6** (1.751 and 1.930 Å).

The major discrepancies in the hydrogen-bonding network between these compounds (**4–7**) can be better understood by viewing the superimposed structures and observing the orientation of the critical OH groups (Figure 7). With the exception of the equatorial 3'-OH in north-diazepinone **5** (yellow), the axial orientations of the 3'-OH in the rest of the molecules remains in close proximity. There is good freedom of rotation for the CH₂OH group in **5**, which allows it to reach a new amino acid, Leu142, to compensate for the lack of interaction with Ala58 and Tyr60 seen with the rest of the compounds. The diazepinone ring appears perfectly superimposed in all four structures. The 2'-OH is present only in the parent riboside **4** but this group appears not to be engaged in any important interaction, thus supporting the equivalent affinity that CDA displays for both ribo and 2'-deoxyribonucleosides (substrates or inhibitors).

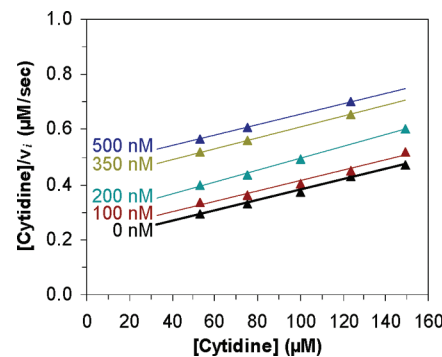


FIGURE 5. Hanes plot for cytidine deaminase activity at various concentrations (defined in the figure) of the flexible diazepinone inhibitor **7** (▲). The parallel lines represent linear fits to the data and are indicative of competitive inhibition.

TABLE 1. Inhibition Constants for Carbocyclic Diazepinones

compd	K_i (μM)
north-diazepinone (5)	70 ± 10
south-diazepinone (6)	40 ± 10
flexible-diazepinone (7)	0.4 ± 0.1

Discussion

The selection of the diazepinone riboside **4** as a prototype to study the preferred conformation of CDA for a particular sugar pucker was based on the premise that the newly revealed edge-on $\pi-\pi$ interaction between the diazepinone ring's double bond and Phe137⁷ provided a mechanism of inhibition independent of the zinc-promoted hydration for which the role of the sugar O4' oxygen would not be considered critical. In the case of the mechanistically related adenosine deaminase (ADA)²⁶ and also for CDA,²⁷ studies with carbocyclic nucleosides in our hands have revealed that the sugar moiety plays a significant role in facilitating zinc-promoted hydration due to the more electronegative nature of the sugar moiety and important orbital interactions between the oxygen's (O4') lone pair with the highest p orbital component and the adjacent C–N glycosyl bond through the anomeric effect. Thus, replacement of the ribose or 2'-deoxyribose ring of adenosine and cytidine with carbocyclic pseudosugars removes any communication between the sugar and the nucleobase and the rates of deamination decrease.²⁷ The diazepinone-based inhibitors (**4–7**), which lack any possibility of interacting with CDA via zinc coordination and work independently of hydration, are therefore ideal candidates to study the effect of sugar (or pseudosugar) ring puckering on the mechanism of CDA.

Because all the crystal structures of bound inhibitors to CDA have shown the conformation of the sugar ring to be in the south hemisphere,^{3c, 3d, 5, 7} close to a 2'-endo conformation, we hypothesized that the conformationally south-locked diazepinone nucleoside **6** would be the most potent inhibitor in comparison with the antipodal north-locked **5**,

(25) Macromodel 9.5, Schrodinger, LLC, New York, 2007.

(26) Marquez, V. E.; Russ, P.; Alonso, R.; Siddiqui, M. A.; Hernandez, S.; George, C.; Nicklaus, M. C.; Dai, F.; Ford, H., Jr. *Helv. Chim. Acta* **1999**, 82, 2119–2129.

(27) Marquez, V. E.; Schroeder, G. K.; Ludek, O. R.; Siddiqui, M. A.; Ezzitouni, A.; Wolfenden, R. *Nucleosides, Nucleotides Nucleic Acids*, in press.

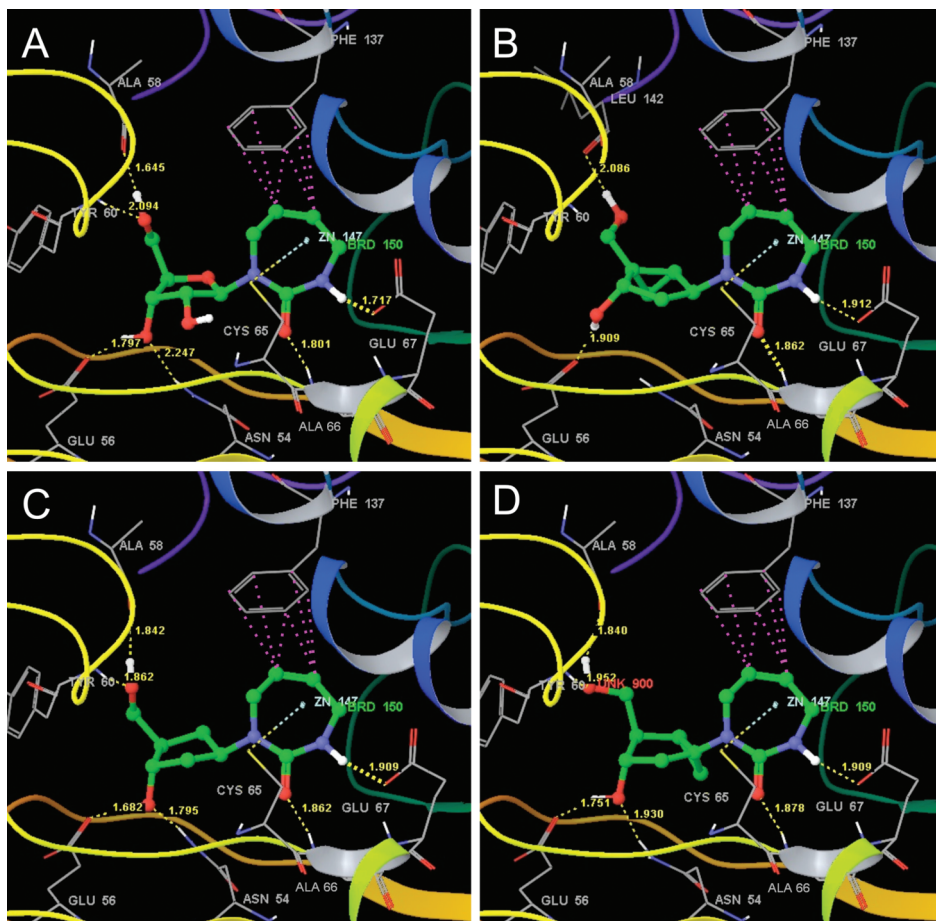


FIGURE 6. Monte Carlo/Stochastic Dynamics simulations in MacroModel 9.5²⁵ of four diazepinone compounds in human cytidine deaminase: (A) diazepinone riboside (**4**, conformation in the crystal structure); (B) north-diazepinone (**5**); (C) flexible diazepinone (**7**); (D) south-diazepinone (**6**). Hydrogen bonds appear as yellow dashed lines, and the canonical π/π interaction with the π -face of Phe137 is represented by a group of purple dotted lines. As a reference point, the atom of zinc appears bonded to Cys65.

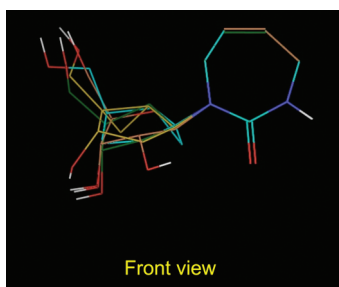


FIGURE 7. Overlapping of CDA-bound conformation of **4** (khaki), **5** (yellow), **6** (cyan), and **7** (green).

and the flexible diazepinone nucleoside **7**. As mentioned before, the preference of CDA for the south (2'-endo) conformation is in sharp contrast with that of ADA, which prefers to bind both substrate and inhibitors in the antipodal north (3'-endo) conformation.¹² This unique preference for an antipodal sugar puckering by CDA is another important element of differentiation from the seemingly similar ADA.

The biochemical results from this investigation indeed confirm CDA's preference for a south sugar conformation since the south inhibitor **6** was more potent than its north counterpart **5** albeit only by a factor of ~ 2 (Table 1).

Surprisingly, the flexible cyclopentane diazepinone nucleoside **7** was more potent than the south-diazepinone **6** by a factor of 100 (Table 1). However, relative to the normal riboside (**4**), the flexible diazepinone **7** was only 16-fold less potent. A likely explanation for the less than expected performance of the south-diazepinone nucleoside **6** stems from the fusion of the cyclopropane ring adjacent to the glycosyl C–N bond. As the crystal structures of CDA in complex with THU and diazepinone riboside **4** show, the glycosyl torsion angles ($\chi = -136.51^\circ$ and $\chi = -149.66^\circ$) are clearly in the anti range. Unfortunately, as we have observed with all pyrimidine nucleosides built on a south-bicyclo-[3.1.0]hexane pseudosugar template, both single-crystal X-ray structures and ab initio calculations have shown that the glycosyl torsion angle is more stable in the syn region.²⁸ This means that the enzyme has to pay a significant penalty to accommodate the inhibitor in the less stable anti conformation. Despite this shortcoming, the south-diazepinone **6** was still able to inhibit CDA more effectively than its north counterpart. However, the penalty incurred in changing the conformation from syn to anti inside a binding pocket that is completely sequestered from bulk solvent diminishes the

(28) Marquez, V. E.; Ben-Kasus, T.; Barchi, J. J., Jr.; Green, K. M.; Nicklaus, M. C.; Agbaria, R. *J. Am. Chem. Soc.* **2004**, *126*, 543–549.

capacity of CDA to discriminate effectively between the two inhibitors on the basis of ring pucker.

The same argument can explain the 100-fold difference between the flexible diazepinone **7** and the south-diazepinone **6**, which as seen in parts C and D of Figure 6 fit almost identically. The flexible diazepinone does not have a constrained syn glycosyl torsion angle since the plastic cyclopentane ring can easily reach the *P* value observed for the ribose ring in **4** (*P* = 158.18°) at the active site of CDA. If we take as a reference the approximate 1'-exo (*P* = 118.6°) conformation found in the crystal structure of plain carbocyclic thymidine,²⁹ the cyclopentane ring in **7** has to change its puckering 40° (pseudorotational degrees) to reach the 2'-endo conformation. This change is very much achievable in solution and with a much lower energy penalty when compared to that required to rotate the glycosyl bond in **6**. This small penalty in changing ring puckering could very well reflect the 16-fold lower potent inhibition of CDA by **7** relative to the parent ribose **4**.

To strengthen our argument that the effective north/south discrimination by CDA was weakened by the syn-preference of the south-locked diazepinone **6**, we performed a conformational analysis by sampling the entire conformational space of χ from 0° to 360° (Figure 8) as we have done previously for the locked north- and south-thymidine analogues.²⁸ For the locked south-thymidine analogue, which has the same bicyclo[3.1.0]hexane scaffold of **6**, a relative energy barrier of ~17 kcal/mol separated the most stable syn conformer (χ = ~60°) from the less stable anti conformer (χ = ~−120°). The energy barrier for the larger, bulkier diazepinone ring was somewhat higher (~18 kcal/mol), reflecting a greater difficulty in achieving the anti conformation demanded by the enzyme. Furthermore, the anti conformer for **6** was significantly less stable than the corresponding south-locked thymidine anti conformer. As in the case of the south-locked thymidine analogue, the integrity of the bicyclo[3.1.0]hexane system remained constant during the calculations as indicated by the small variance of *P* across the entire range (not shown).

In conclusion, the observed order of inhibitory potency **4** > **7** > **6** > **5** can be easily explained in terms of two important factors: (1) the preferred sugar puckering of CDA for the south conformation and (2) the preferred anti disposition of the base bound at the active site. The small ~2-fold difference between south-locked **6** and north-locked **5** suggests that the most efficient network of hydrogen bonds provided by the south template allows CDA to overcome the penalty incurred in rotating χ from syn to anti and differentiate between the two. However, this penalty becomes an important issue when comparing the south-locked **6** with the flexible-diazepinone **7**, for which such a penalty no longer exists, allowing the ring to reach the required 2'-endo pucker with relative ease from its preferred 1'-exo conformation. These conformational issues could explain the 100-fold separation in potency observed between these two compounds. Finally, the diazepinone-riboside **4** also does not incur the penalty of rotating χ , and by its very nature, the ribose ring has a very small energy barrier separating the 3'-endo from the precise 2'-endo conformation required for

(29) Kalman, A.; Koritsanszky, T.; Beres, J.; Sagi, G. *Nucleosides Nucleotides* **1990**, *9*, 235–243.

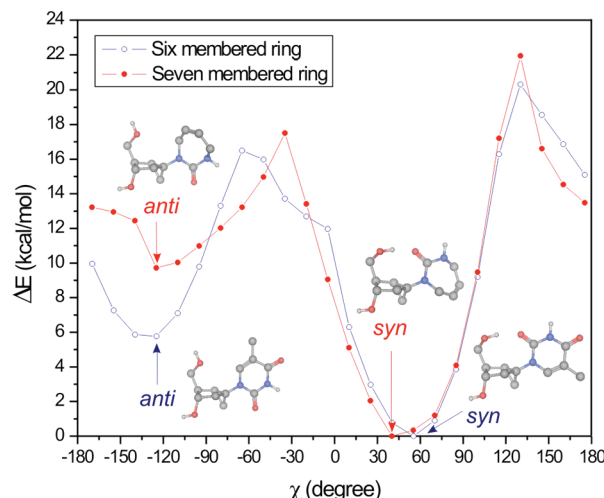


FIGURE 8. Ab initio potential energy scan (PES) of south-locked diazepinone **6** and south-locked thymidine (six-membered ring).

binding. We can therefore conclude that in accordance to the structural information gathered from X-ray crystallography our set of inhibitors prove that CDA indeed has a penchant for the south conformation, which is opposite to that of ADA. One final point of interest in cancer chemotherapy regarding the combined use of antitumor nucleosides that are readily deaminated by CDA is that the very stable and quite potent carbocyclic diazepinone nucleoside (**7**) could overcome many of the instability problems associated with the use of tetrahydrouridine (THU, **3**).³⁰

Experimental Section

Molecular Modeling. Molecular dynamics calculations were performed using the Monte Carlo/Stochastic Dynamics (MC/SD) program available in MacroModel 9.5²⁵ to simulate molecular movement over time using Newton's equation of motion. This program performs constant temperature calculations that take advantage of the strengths of the Monte Carlo method for quickly introducing large changes in a few degrees of freedom and stochastic dynamic for an effective local sampling of collective motions. For these calculations, the OPLS_2005 force field was employed and water was used as a solvent. To force the system to meet the desired geometrical conditions and to reduce the cost of computer time by eliminating calculations expected to have little influence on the results, all residues that do not have any atoms within 6 Å of the ligands and the seven atoms of the diazepinone ring were fixed. The maximum iterations and convergence threshold were set to 5000 and 0.00, respectively. The number of structures to sample was set to 10, and the simulation time was 100 ps.

Ab Initio Potential Energy Scans (PES). The structure of the south-locked thymidine analogue (entry code: YESMIS³¹) was taken from the Cambridge Structural Database.^{32,33} Since YESMIS is a dimer containing two conformers, one of them was taken for further ab initio calculations. The structure of compound **6** was built from two segments, the sugar ring extracted from YESMIS and the diazepinone ring extracted from the PDB file

(30) Kelley, J. A.; Driscoll, J. S.; McCormack, J. J.; Roth, J. S.; Marquez, V. E. *J. Med. Chem.* **1986**, *29*, 2351–2358.

(31) Altmann, K. H.; Imwinkelried, R.; Kesselring, R.; Rihs, G. *Tetrahedron Lett.* **1994**, *35*, 7625–7648.

(32) Allen, F. H. *Acta Crystallogr B* **2002**, *58*, 380–388.

(33) Bruno, I. J.; Cole, J. C.; Edgington, P. R.; Kessler, M.; Macrae, C. F.; McCabe, P.; Pearson, J.; Taylor, R. *Acta Crystallogr B* **2002**, *58*, 389–397.

1MQ0.⁷ The structure of **6** was first minimized, and then a conformational search was performed employing the Systematic Search method in MOE 2007.09.³⁴ The identified global energy minimum conformation was then used for ab initio calculations. Both the south-locked thymidine and **6** were preoptimized at the HF/3-21G level of theory and then reoptimized at the HF/6-311G level in the program Gaussian 03, revision E01 (Gaussian, Inc.). The two structures, which were assumed to be local or global energy minima, were investigated by performing a PES of the dihedral angle χ by rotating the base in steps of 15°. Using the Gaussian HF method at the same 6-311G level of theory, each of the geometries obtained were optimized for all internal coordinates, except the dihedral angle χ .

Cytidine Deaminase Inhibition. Cytidine deaminase from *E. coli* was purified as previously described.^{3a} Enzymatic activity (~1 nM CDA) was measured spectrophotometrically in 1 mL cuvettes by following the loss of absorbance of cytidine at 282 nm ($\Delta\epsilon = -3600$) in 0.1 M phosphate buffer (pH 6.8) at 25 °C. Concentrations of stock solutions of the three carbocyclic diazepinones (**5–7**) were determined by proton NMR (see Figures 2–4 in the Supporting Information) in reference to a known concentration of pyrazine (10^{-3} M) added as an integration standard.

((1R,2S,4S,5S)-2-Acetoxy-4-azidobicyclo[3.1.0]hexan-1-yl)methyl Acetate (10) (Method A). To a stirred solution of alcohol **8** (850 mg, 3.72 mmol) in dry DMF (25 mL) were added diphenyl-phosphoryl azide (DPPA, 2.40 mL, 11.2 mmol) and triethylamine (1.80 mL, 13.0 mmol) under argon at room temperature. The mixture was warmed to 60 °C and stirred for 20 h. The solvent was evaporated, and the residue was partitioned between water (50 mL) and CH₂Cl₂ (50 mL). After phase separation, the aqueous phase was extracted again with CH₂Cl₂ (2 × 50 mL), and the combined extracts were dried (Na₂SO₄) and concentrated. The crude material was purified by flash chromatography on silica gel (EtOAc in hexanes 25–45%) to yield the azide **10** (706 mg, 75%) as a colorless oil: [α]²⁰_D −57.71 (c 0.78, CHCl₃); IR (neat) 3014, 2098, 1733, 1631, 1370, 1230, 1025, 973, 905, 835 cm^{−1}; ¹H NMR (400 MHz, CDCl₃) δ 5.49 (app t, 1H, J ≈ 8.8 Hz, H-2), 4.22 (d, 1H, J = 12.0 Hz, CHH-OAc), 3.97 (d, 1H, J = 12.0 Hz, CHH-OAc), 3.81 (d, 1H, J = 6.2 Hz, H-4), 2.25 (ddd, 1H, J = 14.8, 8.1, 1.0 Hz, H-3a), 2.09 (s, 3H, OAc), 1.99 (s, 3H, OAc), 1.53 (dd, 1H, J = 8.6, 4.3 Hz, H-5), 1.41 (ddd, 1H, J = 14.8, 8.4, 6.2 Hz, H-3b), 0.84 (dd, 1H, J = 6.2, 4.3 Hz, H-6a), 0.79–0.75 (m, 1H, H-6b); ¹³C NMR (100 MHz, CDCl₃) δ 171.0, 70.8 (2 × C=O, Ac), 74.7 (C-2), 65.1 (CH₂-OAc), 61.5 (C-4), 34.5 (C-3), 30.8 (C-1), 26.5 (C-5), 20.9, 20.8 (2 × CH₃, Ac), 11.1 (C-6); FAB-MS *m/z* (relative intensity) 254 (45), 194 (100). Anal. Calcd for C₁₁H₁₅N₃O₄: C, 52.17; H, 5.97; N, 16.59. Found: C, 52.26; H, 6.01; N, 16.35.

((1R,2S,4S,5S)-2-Acetoxy-4-azidobicyclo[3.1.0]hexan-1-yl)methyl Acetate (10) (Method B). The bicyclic hexanol **8** (600 mg, 2.36 mmol) was dissolved in dry CH₂Cl₂ (20 mL) under argon at 0 °C, and triethylamine (1.10 mL, 7.89 mmol) and methansulfonyl chloride (MsCl, 305 μL, 3.94 mmol) were slowly added. The reaction mixture was stirred for 1 h at 0 °C and then poured into a mixture of ice-cold phosphate buffer (pH, 7.2, 150 mL) and Et₂O (150 mL). The aqueous phase was extracted with Et₂O (2 × 100 mL), and the combined extracts were dried (MgSO₄) and concentrated. The crude mesylate **9** was used in the next substitution reaction without any further purification (decomposition occurred during chromatography on silica gel): IR (neat) 3019, 2941, 1733, 1446, 1351, 1237, 1171, 1032, 970, 922, 846 cm^{−1}; ¹H NMR (400 MHz, CDCl₃) δ 5.20–5.11 (m, 2H, H-2, H-4), 4.20 (d, 1H, J = 12.0 Hz, CHH-OAc), 3.78 (d, 1H, J = 12.0 Hz, CHH-OAc), 2.94 (s, 3H, CH₃-SO₃), 2.63 (ddd, 1H, J = 14.1, 7.8, 7.8 Hz, H-3a), 1.99 (s, 3H, OAc), 1.98 (s, 3H, OAc), 1.83–1.78 (m, 1H, H-3b), 1.25 (dd, 1H, J = 6.0, 4.3 Hz, H-6a),

0.81 (app t, 1H, J ≈ 7.0 Hz, H-6b); FAB-MS *m/z* (relative intensity) 307 (5), 247 (24), 211 (100).

The mesylate **9** (810 mg, 2.36 mmol) was dissolved in dry DMF (20 mL), and sodium azide (1.70 g, 23.6 mmol) was added in one portion under argon at room temperature. The mixture was heated to 90 °C for 1 h and allowed to cool to room temperature. The reaction was poured into a mixture of phosphate buffer (pH 7.2, 100 mL) and Et₂O (100 mL), and the aqueous phase was extracted with Et₂O (2 × 100 mL). The combined organic extracts were dried (MgSO₄) and concentrated. Flash chromatography on silica gel (EtOAc in hexanes 25–45%) yielded the azide **10** (436 mg, 73%) as a colorless oil. The spectral data were identical to those reported above.

((1R,2S,4S,5S)-2-Acetoxy-4-aminobicyclo[3.1.0]hexan-1-yl)methyl Acetate (11). Azide **10** (690 mg, 2.72 mmol) was dissolved in MeOH (25 mL) and CH₂Cl₂ (25 mL) under argon at room temperature, and Lindlar's catalyst (100 mg) was added. The mixture was flushed with hydrogen and stirred at room temperature overnight. The mixture was filtered over a short pad of Celite, and the solvent was evaporated off. The crude amine **11** (618 mg, 100%) was obtained as a colorless wax, which was sufficiently pure to be used in the next step without any further purification. An analytical sample was prepared by flash chromatography on silica gel (MeOH in EtOAc 10–40%): [α]²⁰_D −19.21 (c 0.36, CHCl₃); IR (neat) 3332, 2947, 1729, 1654, 1548, 1370, 1238, 1025, 733 cm^{−1}; ¹H NMR (400 MHz, CDCl₃) δ 5.45 (app t, 1H, J ≈ 8.3 Hz, H-2), 4.17 (d, 1H, J = 11.6 Hz, CHH-OAc), 3.92 (d, 1H, J = 11.6 Hz, CHH-OAc), 3.15 (d, 1H, J = 6.0 Hz, H-4), 2.40–2.10 (bs, 2H, NH₂), 1.94 (s, 3H, OAc), 1.92 (s, 3H, OAc), 1.74 (dd, 1H, J = 13.5, 8.0 Hz, H-3a), 1.30–1.22 (m, 2H, H-3b, H-5), 0.72 (app t, 1H, J ≈ 4.8 Hz, H-6a), 0.62 (dd, 1H, J = 8.2, 5.5 Hz, H-6b); ¹³C NMR (100 MHz, CDCl₃) δ 171.5, 171.4 (2 × C=O, Ac), 75.9 (C-2), 66.4 (CH₂-OAc), 51.2 (C-4), 36.2 (C-3), 30.2 (C-1), 29.5 (C-5), 19.5, 19.4 (2 × CH₃, Ac), 10.4 (C-6); FAB-MS *m/z* (relative intensity) 228 (100), 186 (38). Anal. Calcd for C₁₁H₁₇NO₄·0.2H₂O: C, 57.23; H, 7.60; N, 6.07. Found: C, 57.08; H, 7.59; N, 5.86.

((1R,2S,4S,5S)-2-Acetoxy-4-allylaminobicyclo[3.1.0]hexan-1-yl)methyl Acetate (12) and ((1R,2S,4S,5S)-2-Acetoxy-4-diallylamino-bicyclo[3.1.0]hexan-1-yl)methyl Acetate (13). The amine **11** (100 mg, 0.440 mmol) was dissolved in dry DMF (2.0 mL) at room temperature, and potassium carbonate (anhydrous, 166 mg, 1.20 mmol) was added in one portion under argon. Allyl bromide was slowly added at room temperature and the mixture was stirred overnight. The solvent was evaporated off, and the residue was chromatographed on silica gel (MeOH in EtOAc 0–10%) to yield the title compound **12** (40.1 mg, 35%) as a colorless oil, together with the dialkylated derivative **13** (33.8 mg, 25%).

Compound **12**: [α]²⁰_D 3.54 (c 0.58, CHCl₃); IR (neat) 3323, 2946, 1731, 1643, 1457, 1370, 1238, 1111, 1024, 916, 759 cm^{−1}; ¹H NMR (400 MHz, CDCl₃) δ 5.84 (m, 1H, CH=CH₂), 5.49 (app t, 1H, J ≈ 8.3 Hz, H-2), 5.13 (ddd, 1H, J = 17.1, 3.0, 1.6 Hz, CH=CHH), 5.04 (ddd, 1H, J = 10.2, 3.0, 1.6 Hz, CH=CHH), 4.18 (d, 1H, J = 12.0 Hz, CHH-OAc), 3.99 (d, 1H, J = 12.0 Hz, CHH-OAc), 3.25–3.15 (m, 2H, CH₂-CH=CH₂), 3.14 (d, 1H, J = 6.2 Hz, H-4), 2.09 (dd, 1H, J = 14.3, 8.3 Hz, H-3a), 2.00 (s, 3H, OAc); 1.99 (s, 3H, OAc), 1.64–1.59 (bs, 1H, NH), 1.40 (dd, 1H, J = 8.4, 4.4 Hz, H-5), 1.26 (m, 1H, H-3b), 0.82 (dd, 1H, J = 5.6, 4.4 Hz, H-6a), 0.68 (dd, 1H, J = 8.4, 5.6 Hz, H-6b); ¹³C NMR (100 MHz, CDCl₃) δ 171.1 (2 × C=O, OAc), 136.6 (CH=CH₂), 115.8 (CH=CH₂), 76.0 (C-2), 66.2 (CH₂-OAc), 57.5 (CH₂-CH=CH₂), 49.6 (C-4), 34.2 (C-3), 30.1 (C-1), 28.2 (C-5), 21.1, 20.9 (2 × CH₃, OAc), 11.2 (C-6); FAB-MS *m/z* (relative intensity) 268 (100), 208 (30). Anal. Calcd for C₁₄H₂₁NO₄: C, 62.90; H, 7.92; N, 5.24. Found: C, 62.81; H, 7.96; N, 5.02.

Compound **13**: ¹H NMR (400 MHz, CDCl₃) δ 5.73–5.78 (m, 1H, CH=CH₂-A), 5.72–5.68 (m, 1H, CH=CH₂-B), 5.39 (app t,

(34) MOE, version 2007.09, Chemical Computing Group, Montreal, Quebec, Canada. 2007.

1H, $J \approx 8.3$ Hz, H-2), 5.13 (dd, 1H, $J = 3.0, 1.7$ Hz, CH=CHH-A), 5.08 (dd, 1H, $J = 3.0, 1.6$ Hz, CH=CHH-A), 5.05 (br dd, 1H, CH=CHH-B), 5.02 (br dd, 1H, CH=CHH-B), 4.26 (d, 1H, $J = 12.0$ Hz, CHH-OAc), 3.89 (d, 1H, $J = 12.0$ Hz, CHH-OAc), 3.38 (d, 1H, $J = 7.9$ Hz, H-4), 3.20 (ddd, 2H, $J = 14.0, 5.4, 1.5$ Hz, CH₂-allyl-A), 2.80 (dd, 2H, $J = 14.0, 7.3$ Hz, CH₂-allyl-B), 2.24 (dd, 1H, $J = 15.1, 8.5$ Hz, H-3a), 1.98 (s, 3H, OAc), 1.95 (s, 3H, OAc), 1.34 (dd, 1H, $J = 7.5, 5.4$ Hz, H-5), 1.22–1.14 (m, 1H, H-3b), 0.69–0.64 (m, 2H, 6-CH₂); ¹³C NMR (100 MHz, CDCl₃) δ 170.9 (2 \times C=O, OAc), 136.6 (2 \times CH=CH₂), 117.0 (2 \times CH=CH₂), 76.4 (C-2), 66.1 (CH₂-OAc), 60.8 (2 \times CH₂-CH=CH₂), 53.1 (C-4), 31.7 (C-3), 30.8 (C-1), 26.5 (C-5), 21.1, 20.8 (2 \times CH₃, Ac), 11.4 (C-6); ESI-MS (*m/z*) 308.2 (M + H⁺).

((1R,2S,4S,5S)-2-Acetoxy-4-(*tert*-butoxycarbonylamino)bicyclo[3.1.0]hexan-1-yl)methyl Acetate (14). Azide 11 (1.20 g, 4.74 mmol) was dissolved in CH₂Cl₂, and di-*tert*-butyl dicarbonate ((Boc)₂O, 1.24 g, 5.69 mmol) was added at room temperature under argon. The hydrogenation catalyst (Pd/C, 10%, 150 mg) was added, and the mixture was flushed with H₂ and stirred at room temperature until all starting material was consumed by TLC analysis. The solvent was filtered through a short pad of Celite, and the filtrate was concentrated. The crude was purified by flash chromatography on silica gel (EtOAc in hexanes 20–40%) to yield the carbamate 14 (1.46 g, 94%) as a colorless oil: [α]²⁰_D 7.59 (c 0.83, CHCl₃); IR (neat) 3345, 2976, 1707, 1518, 1454, 1364, 1237, 1166, 1038, 974, 905, 853, 783 cm⁻¹; ¹H NMR (400 MHz, CDCl₃) δ 5.47 (app t, 1H, $J \approx 8.4$ Hz, H-2), 4.57 (br s, 1H, NH), 4.27 (d, 1H, $J = 11.8$ Hz, CHH-OAc), 4.04–3.98 (m, 1H, H-4), 3.92 (d, 1H, $J = 11.8$ Hz, CHH-OAc); 2.11 (dd, 1H, $J = 14.4, 8.0$ Hz, H-3a); 2.05 (s, 3H, OAc); 2.02 (s, 3H, OAc), 1.47–1.37 (m, 1H, H-3b, H-5, *t*-Bu, Boc), 0.89 (dd, 1H, $J = 6.0, 4.4$ Hz, H-6a), 0.72 (dd, 1H, $J = 8.4, 6.0$ Hz, H-6b); ¹³C NMR (100 MHz, CDCl₃) δ 171.1, 170.9 (2 \times C=O, OAc), 154.8 (C=O, Boc), 79.6 (C(CH₃)₃, Boc), 74.9 (C-2), 65.8 (CH₂-OAc), 51.1 (C-4), 35.4 (C-1), 30.2 (C-3), 28.4 (C(CH₃)₃, Boc), 27.7 (C-5), 21.0, 20.9 (2 \times CH₃, OAc), 11.0 (C-6); FAB-MS *m/z* (relative intensity) 328 (3.7), 212 (100). Anal. Calcd for C₁₆H₂₅NO₆: C, 58.70; H, 7.70; N, 4.28. Found: C, 58.25; H, 7.70; N, 4.19.

((1R,2S,4S,5S)-2-Acetoxy-4-(allyl-*tert*-butoxycarbonylamino)bicyclo[3.1.0]hexan-1-yl)methyl Acetate (15). To a stirred solution of carbamate 14 (350 mg, 1.07 mmol) in dry DMF (14.0 mL) were added KHMDS (0.5 M in toluene, 2.57 mL, 1.28 mmol) and allyl bromide (120 μ L, 1.39 mmol) at 0 °C under argon. The mixture was continued to stir for 5 h at 0 °C and then poured into a mixture of phosphate buffer (100 mL, pH 7.2) and Et₂O (100 mL). The aqueous phase was further extracted with Et₂O (2 \times 100 mL), and the combined organic phases were dried (Na₂SO₄) and concentrated. The crude residue was purified by flash chromatography (EtOAc in hexanes 20–40%) to yield the title compound 15 (252 mg, 64%) as a colorless oil: [α]²⁰_D 3.31 (c 1.16, CHCl₃); IR (neat) 2976, 1736, 1687, 1454, 1364, 1330, 1237, 1170, 1143, 1023, 910, 776 cm⁻¹; ¹H NMR (400 MHz, CDCl₃) δ 5.81 (m, 1H, CH=CH₂), 5.54 (app t, 1H, $J \approx 8.4$ Hz, H-2), 5.16–5.06 (m, 2H, CH=CH₂), 4.16 (br s, 1H, H-4), 4.35 (d, 1H, $J = 12.0$ Hz, CHH-OAc), 3.89 (d, 1H, $J = 12.0$ Hz, CHH-OAc), 3.81 (br s, 2H, CH₂-CH=CH₂), 2.16 (dd, 1H, $J = 15.3, 8.5$ Hz, H-3a), 2.03 (s, 3H, OAc), 2.00 (s, 3H, OAc), 1.62–1.54 (m, 1H, H-3b), 1.41 (s, 9H, *t*Bu), 1.37 (dd, 1H, $J = 8.8, 4.3$ Hz, H-5), 0.77 (dd, 1H, $J = 5.8, 4.3$ Hz, H-6a), 0.71 (dd, 1H, $J = 8.8, 5.8$ Hz, H-6b); ¹³C NMR (100 MHz, CDCl₃) δ 171.1, 170.8 (2 \times C=O, Ac), 155.1 (C=O, BOC), 135.9 (CH=CH₂), 115.2 (CH=CH₂), 79.8 (O-C(CH₃)₃), 75.5 (C-2), 65.9 (CH₂-OAc), 56.3 (CH₂-CH=CH₂), 45.6 (C-4), 36.1 (C-3), 32.2 (C-1), 28.4 (O-C(CH₃)₃), 26.8 (C-5), 21.0, 20.8 (2 \times CH₃, Ac), 11.2 (C-6); FAB-MS *m/z* (relative intensity) 368 (5), 252 (100). Anal. Calcd for C₁₉H₂₉NO₆: C, 62.11; H, 7.96; N, 3.81. Found: C, 62.36; H, 7.89; N, 3.79.

((1R,2S,4S,5S)-2-Acetoxy-4-allylaminobicyclo[3.1.0]hexan-1-yl)methyl Acetate (12). The Boc-protected amine 15 (250 mg,

0.680 mmol) was dissolved in anhydrous CH₂Cl₂ (15 mL), and TFA (2.5 mL) was added at 0 °C under argon. After the addition, the mixture was continued to stir at 0 °C and frequently monitored by TLC (CH₂Cl₂–MeOH 9:1). After the mixture was stirred for 3 h at 0 °C, all starting material was consumed and satd NaHCO₃ (50 mL) was carefully added while the mixture was vigorously stirred. The layers were separated, and the aqueous phase was extracted with CH₂Cl₂ (2 \times 50 mL). The combined extracts were dried (MgSO₄) and concentrated. The crude product was sufficiently pure (by TLC, ¹H NMR) to be used without any further purification in the next step. The spectroscopic data were identical to those reported above.

((1R,2S,4S,5S)-2-Acetoxy-4-(1,3-diallylureido)bicyclo[3.1.0]-hexan-1-yl)methyl Acetate (16). The allyl amine 12 (260 mg, 0.973 mmol) was dissolved in anhydrous CH₂Cl₂ (20 mL) and cooled to –20 °C under argon. Allyl isocyanate (162 mg, 1.38 mmol) was slowly added, and the mixture was gradually warmed to room temperature and stirred overnight. The solvent was evaporated off under reduced pressure, and the residue was purified by flash chromatography (silica gel, EtOAc in hexanes 60–80%) to yield the urea 16 (307 mg, 93%) as a colorless oil: [α]²⁰_D 4.94 (c 0.89, CHCl₃); IR (neat) 3430, 3366, 3079, 2982, 1734, 1637, 1522, 1370, 1237, 1024, 915, 850 cm⁻¹; ¹H NMR (400 MHz, CDCl₃) δ 5.85–5.75 (m, 2H, 2 \times CH=CH₂), 5.49 (app t, 1H, $J \approx 8.5$ Hz, H-2), 5.30–5.20 (m, 2H, 2 \times CH=CHH), 5.10–5.00 (m, 2H, 2 \times CH=CHH), 4.87 (d, 1H, $J = 8.1$ Hz, H-4), 4.49 (t, 1H, $J = 5.4$ Hz, NH), 4.35 (d, 1H, $J = 12.0$ Hz, CHH-OAc), 3.84–3.75 (m, 5H, CHH-OAc, 2 \times CH₂-CH=CH₂), 2.09 (dd, 1H, $J = 15.5, 8.8$ Hz, H-3a), 1.98 (s, 6H, 2 \times OAc), 1.66–1.58 (m, 1H, H-3b), 1.30 (dd, 1H, $J = 8.8, 4.4$ Hz, H-5), 0.77 (dd, 1H, $J = 5.9, 4.4$ Hz, H-6a), 0.70 (dd, 1H, $J = 8.8, 5.9$ Hz, H-6b); ¹³C NMR (100 MHz, CDCl₃) δ 171.1, 170.7 (2 \times C=O, Ac), 157.9 (C=O, urea), 135.7, 135.4 (2 \times CH=CH₂), 116.8, 115.4 (2 \times CH=CH₂), 75.3 (C-2), 65.9 (CH₂-OAc), 55.7 (C-4), 45.6, 43.2 (2 \times CH₂-allyl), 36.3 (C-3), 32.2 (C-1), 26.9 (C-5), 21.0, 20.8 (2 \times CH₃, Ac), 11.3 (C-6); FAB-MS *m/z* (relative intensity) 351 (15), 291 (100). Anal. Calcd for C₁₈H₂₆N₂O₅: C, 61.70; H, 7.48; N, 7.99. Found: C, 61.60; H, 7.68; N, 7.86.

((1'R,2'S,4'S,5'S)-2'-Acetoxy-4'-(2-oxo-2,3-dihydropyrimidin-1(6*H*)-yl)bicyclo[3.1.0]hexan-1-yl)methyl Acetate (20). Urea 16 (20.0 mg, 0.057 mmol) was dissolved in hexamethyldisilazane (HMDS, 1.0 mL), and a catalytic amount of ammonium sulfate was added. The mixture was heated to reflux for 2 h and cooled to room temperature. The solvent was removed in vacuo, and the residue was dissolved in anhydrous and deoxygenated CH₂Cl₂ (5 mL). Grubbs second-generation catalyst (4.8 mg, 5.65 μ mol) was added. The mixture was heated to reflux for 1 h and cooled to room temperature. The solvent was evaporated off, and the residue was purified by flash chromatography on silica gel (EtOAc in hexanes, 60–80%) to yield the six-membered urea 20 (12.5 mg, 71%) as a brown foam. The sample was still contaminated with tricyclohexylphosphineoxide resulting from catalyst decomposition: ¹H NMR (400 MHz, CDCl₃) δ 6.10–6.00 (br s, 1H, NH), 6.00–6.95 (m, 1H, H-4), 5.48 (app t, 1H, $J \approx 8.4$ Hz, H-2'), 4.99 (d, 1H, $J = 8.2$ Hz, H-4'), 4.69–4.66 (m, 1H, H-5), 4.30 (d, 1H, $J = 12.0$ Hz, CHH-OAc), 3.98 (ddd, 1H, $J = 14.3, 3.2, 1.3$ Hz, H-6a), 3.90 (d, 1H, $J = 12.0$ Hz, CHH-OAc), 3.79 (ddd, 1H, $J = 14.3, 3.2, 1.7$ Hz, H-6b), 2.14 (dd, 1H, $J = 15.6, 8.4$ Hz, H-3'a), 1.99 (s, 3H, CH₃, OAc), 1.98 (s, 3H, CH₃, OAc), 1.64–1.56 (m, 1H, H-3'b), 1.30 (dd, 1H, $J = 8.6, 4.4$ Hz, H-5'), 0.77–0.70 (m, 2H, H-6'a, b); ¹³C NMR (100 MHz, CDCl₃) δ 171.2, 170.7 (2 \times C=O, Ac), 153.4 (C-2), 124.8 (C-4), 96.6 (C-5), 75.8 (C-2'), 65.8 (CH₂-OAc), 54.1 (C-4'), 41.2 (C-6), 34.1 (C-3'), 32.0 (C-1'), 25.8 (C-5'), 21.0, 20.8 (2 \times CH₃, Ac), 11.0 (C-6'); FAB-MS *m/z* (relative intensity) 309 (32), 249 (100), 297 (tricyclohexylphosphineoxide, 71).

((1R,2S,4S,5S)-2-Acetoxy-4-(1,3-diallyl-3-benzoylureido)bicyclo[3.1.0]hexan-1-yl)methyl Acetate (21). Urea 16 (140 mg, 0.400 mmol)

was dissolved in dry pyridine (3.5 mL) at 0 °C under argon, and triethylamine (168 μ L, 1.20 mmol) and benzoyl chloride (140 μ L, 1.20 mmol) were added dropwise. The mixture was allowed to warm to room temperature and was stirred for 3 h. The solvent was evaporated off, and the residue was partitioned between CH_2Cl_2 (50 mL) and 1 N HCl (50 mL). The aqueous phase was further extracted with CH_2Cl_2 (2 \times 50 mL), and the combined extracts were dried (MgSO_4) and concentrated. The crude was purified by flash chromatography on silica gel (EtOAc in hexanes 50–70%) to yield the *N*-acylurea **21** (162 mg, 89%) as a colorless syrup: $[\alpha]^{20}_{\text{D}} -6.57$ (*c* 1.06, CHCl_3); IR (neat) 3088, 2948, 2252, 1736, 1674, 1648, 1578, 1412, 1369, 1238, 1195, 1025, 915, 795 cm^{-1} ; ^1H NMR (400 MHz, CDCl_3) δ 7.62–7.58 (m, 2H, *CH*-arom), 7.47–7.42 (m, 1H, *CH*-arom), 7.38–7.32 (m, 2H, *CH*-arom), 5.94–5.84 (m, 1H, $\text{CH}=\text{CH}_2$ -A), 5.66–5.56 (m, 1H, $\text{CH}=\text{CH}_2$ -B), 5.41 (app t, 1H, *J* \approx 8.3 Hz, H-2), 5.30–5.10 (m, 4H, $\text{CH}=\text{CH}_2$ -A, $\text{CH}=\text{CH}_2$ -B), 4.45–4.15 (m, 4H, CH_2CH -A, CHH-OAc , H-4), 3.90–3.60 (m, 3H, CH_2CH -B, CHH-OAc), 1.98 (s, 3H, CH_3 , OAc), 1.96 (s, 3H, CH_3 , OAc), 1.50–1.30 (m, 1H, H-5), 0.65–0.59 (m, 2H, H-6a,b); ^{13}C NMR (100 MHz, CDCl_3) δ 170.8, 170.6 (2 \times $\text{C}=\text{O}$, Ac), 169.4 ($\text{C}=\text{O}$, Bz), 157.8 ($\text{C}=\text{O}$, urea), 134.9, 133.4 (2 \times $\text{CH}=\text{CH}_2$), 132.4, 131.6, 128.3, 128.1 (C-arom), 119.2, 117.7 (2 \times $\text{CH}=\text{CH}_2$), 75.0 (C-3), 67.9 (CH_2OAc), 65.4 (CH_2CH -a), 59.2 (C-1), 49.3 (CH_2CH -b), 35.6 (C-4), 32.8 (C-2), 25.5 (C-5), 20.9, 20.7 (2 \times CH_3 , Ac), 11.1 (C-6); FAB-MS *m/z* (relative intensity) 455 (14), 105 (100). Anal. Calcd for $\text{C}_{25}\text{H}_{30}\text{N}_2\text{O}_6$: C, 66.06; H, 6.65; N, 6.16. Found: C, 65.95; H, 6.33; N, 6.08.

((*R,S*)-2',4'S,5'S)-2'-Acetoxy-4'-(*N*-benzoyl-2-oxo-2,3,4,7-tetrahydro-1*H*-1,3-diazepin-1-yl)bicyclo[3.1.0]hexan-1'-yl)methyl Acetate (22). The *N*-benzoylurea **21** (150 mg, 0.330 mmol) was dissolved in dry and deoxygenated CH_2Cl_2 (50 mL) under argon at room temperature, and second-generation Grubbs catalyst (28.0 mg, 0.033 mmol) was added in one portion. The mixture was heated to reflux for 1 h and cooled to room temperature again. The solvent was evaporated off, and the crude was directly subjected to flash chromatography on silica gel (EtOAc in hexanes 45–65%) to yield the diazepinone **22** (130 mg, 92%) as a colorless foam: $[\alpha]^{20}_{\text{D}}$ 39.21 (*c* 1.00, CHCl_3); IR (neat) 3037, 2960, 2883, 1732, 1677, 1461, 1364, 1235, 1192, 1024, 990, 848 cm^{-1} ; ^1H NMR (400 MHz, CDCl_3) δ 7.50–7.46 (m, 2H, *CH*-arom), 7.43–7.38 (m, 1H, *CH*-arom), 7.36–7.31 (m, 2H, *CH*-arom), 5.90–5.82 (m, 1H, H-6), 5.81–5.70 (m, 1H, H-5), 5.54 (app t, 1H, *J* \approx 8.4 Hz, H-2'), 4.61 (d, 1H, *J* = 8.1 Hz, H-4'), 4.54 (br d, 1H, *J* = 18.5 Hz, H-4a), 4.44 (d, 1H, *J* = 12.0 Hz, CHH-OAc), 4.29 (br d, 1H, *J* = 18.5 Hz, H-4b), 4.11–3.92 (m, 2H, H-7a,b), 3.79 (d, 1H, *J* = 12.0 Hz, CHH-OAc), 2.06–2.01 (m, 1H, H-3'a), 2.05 (s, 3H, OAc), 2.00 (s, 3H, OAc), 1.58 (m, 1H, H-3'b), 1.27 (dd, 1H, *J* = 8.3, 4.8 Hz, H-5'), 0.77–0.70 (m, 2H, H-6'a,b); ^{13}C NMR (100 MHz, CDCl_3)

δ 171.1 ($\text{C}=\text{O}$, Bz), 170.8, 170.6 (2 \times $\text{C}=\text{O}$, Ac), 158.8 (C-2), 135.2, 131.4, 128.93, 128.4 (C-arom), 127.1 (C-6), 123.8 (C-5), 74.8 (C-2'), 65.6 (CH_2OAc), 57.0 (C-4'), 43.0 (C-4), 40.8 (C-7), 35.7 (C-1'), 32.4 (C-3'), 26.5 (C-5'), 21.0, 20.9 (2 \times CH_3 , Ac), 11.1 (C-6'); HRMS-FAB *m/z* calcd for $\text{C}_{23}\text{H}_{27}\text{N}_2\text{O}_6$ ($\text{M} + \text{H}^+$) 427.1869, found 427.1856.

1-(*I'S,2'S,4'S,5'R*)-4'-Hydroxy-5'-hydroxymethylbicyclo[3.1.0]-hexan-2'-yl)-3,4-dihydro-1*H*-1,3-diazepin-2(7*H*)-one (5). The fully acylated nucleoside analogue **22** (50.0 mg, 0.117 mmol) was dissolved in a 1% solution of NaOH in methanol (5.0 mL) and stirred at room temperature for 10 min. The mixture was heated to reflux for 1 h and cooled to room temperature again. After neutralization with 2 N HCl, the solvent was evaporated off and the crude was purified by flash chromatography on silica gel (MeOH in EtOAc 5–15%) to yield the diazepinone nucleoside **5** (24.5 mg, 88%) as a colorless foam. The foam was dissolved in acetonitrile/water (1:1, 3 mL) and was lyophyllized to yield a hygroscopic and colorless amorphous semisolid: $[\alpha]^{20}_{\text{D}}$ 16.23 (*c* 1.00, H_2O); IR (neat) 3318, 2869, 1633, 1485, 1428, 1373, 1309, 1190, 1149, 1046, 1007, 846, 786 cm^{-1} ; ^1H NMR (400 MHz, D_2O) δ 5.83–5.76 (m, 1H, H-6), 5.74–5.68 (m, 1H, H-5), 4.65 (t, 1H, *J* = 8.6 Hz, H-4'), 4.27 (d, 1H, *J* = 8.3 Hz, H-2'), 3.85 (d, 1H, *J* = 12.3 Hz, CHH-OH), 3.76 (m, 1H, H-7a), 3.66–3.51 (m, 3H, H-7b, H-6a,b), 3.29 (d, 1H, *J* = 12.3 Hz, CHH-OH), 1.86 (dd, 1H, *J* = 15.3, 8.6 Hz, H-3'a), 1.52 (m, 1H, H-3'b), 1.17 (dd, 1H, *J* = 7.8, 5.1 Hz, H-1'), 0.56–0.52 (m, 2H, H-6'a,b); ^{13}C NMR (100 MHz, D_2O) δ 166.5 (C-2), 128.0 (C-6), 126.3 (C-5), 72.5 (C-4'), 62.9 (CH_2OH), 57.7 (C-2'), 42.2 (C-7), 41.1 (C-5'), 37.4 (C-4), 36.3 (C-3'), 25.6 (C-1'), 9.3 (C-6'); ESI-MS *m/z* 239 ($\text{M} + \text{H}^+$), 261 ($\text{M} + \text{Na}^+$), 277 ($\text{M} + \text{K}^+$). Anal. Calcd for $\text{C}_{12}\text{H}_{18}\text{N}_2\text{O}_3 \cdot 1.0 \text{ H}_2\text{O}$: C, 56.23; H, 7.87; N, 10.93. Found: C, 56.49; H, 7.51; N, 10.59.

Acknowledgment. This research was supported by the Intramural Research Program of the NIH, National Cancer Institute, Center for Cancer Research, and by Grant No. GM-18325 (D.W. and G.K.S.).

Supporting Information Available: Superposition of north-bicyclo[3.1.0]hexane thymidine and south-bicyclo[3.1.0]hexane thymidine adopted in the crystal structures LETJEZ and YES-MIS with docking conformations of **5** and **6**; synthetic methods for the compounds described in Scheme 5; proton NMR spectra (500 MHz) of locked north- and south-diazepinones **5** and **6**, plus flexible diazepinone **7** in D_2O together with internal standard; and ^1H and ^{13}C NMR spectra of new compounds. This material is available free of charge via the Internet at <http://pubs.acs.org>.